



Published in final edited form as:

*J Orthop Res.* 2022 March ; 40(3): 553–564. doi:10.1002/jor.25063.

## Recombinant Fibroblast Growth Factor-18 (Sprifermin), Enhances Microfracture Induced Cartilage Healing

Honey Hendsi<sup>1,#</sup>, Suzanne Stewart<sup>2,#</sup>, Michelle L Gibison<sup>2</sup>, Hans Guehring<sup>4</sup>, Dean W. Richardson<sup>2,#</sup>, George R. Dodge<sup>1,3,\*</sup>

<sup>1</sup>McKay Orthopaedic Research Laboratory, Department of Orthopaedic Surgery, University of Pennsylvania, Philadelphia, PA

<sup>2</sup>Department of Clinical Studies, New Bolton Center, University of Pennsylvania School of Veterinary Medicine

<sup>3</sup>Translational Musculoskeletal Research Center, Corporal Michael J Crescenz VA Medical Center, Philadelphia, PA

<sup>4</sup>Merck KGaA, Darmstadt, Germany

### Abstract

Post-traumatic osteoarthritis is a disabling condition impacting the mostly young and active population. In the present study, we investigated the impact of intra-articular sprifermin, a recombinant truncated fibroblast growth factor 18, on the outcome of microfracture treatment, a widely used surgical technique to enhance cartilage healing at the site of injury.

For this study, we created a cartilage defect and performed microfracture treatment in fetlock joints of 18 horses, treated joints with one of three doses of sprifermin (10, 30, or 100 µg) or with saline, hyaluronan (HA), and evaluated animals functional and structural outcomes over 24 weeks. For primary outcome measures, we performed histological evaluations and gene expression analysis of aggrecan, collagen types I and II, and cartilage oligomeric matrix protein (COMP) in three regions of interest. As secondary outcome measures, we examined animals' lameness, performed arthroscopic, radiographic, and CT scan imaging and gross morphology assessment. We detected the highest treatment benefit following 100 µg sprifermin treatment. The overall histological assessment showed an improvement in the kissing region, and the expression of constitutive genes showed a concentration-dependent enhancement, especially in the peri-lesion area. We detected a significant improvement in lameness scores, arthroscopic evaluations, radiography, and CT scans following sprifermin treatment when results from three dose-treatment groups were combined. Our results demonstrated, for the first time, an enhancement on microfracture outcomes following sprifermin treatment suggesting a cartilage regenerative role and a potential benefit of sprifermin treatment in early cartilage injuries.

### One sentence summary:

\*Corresponding author: George R. Dodge, Ph.D., McKay Orthopaedic Research Laboratory, Department of Orthopaedic Surgery, Perelman School of Medicine, University of Pennsylvania, 379A Stemmler Hall, 36<sup>th</sup> Street and Hamilton Walk, Philadelphia, PA 19104, Phone: (215) 573-1514, Fax: (215) 573-2133, gdodge@pennmedicine.upenn.edu.

#Equal contributions

Fibroblast Growth Factor-18 (Sprifermin) enhanced the outcome of joint microfracture treatment in an equine model suggesting a regenerative role in cartilage healing.

## Keywords

FGF-18; sprifermin; cartilage repair; osteoarthritis; microfracture; equine animal model

## Introduction

Many surgical techniques have been used in an effort to improve healing of major articular cartilage injuries with microfracture probably being the most commonly used.<sup>(1, 2)</sup> In microfracture, small perforations are made into subchondral bone to allow bleeding, and marrow-derived mesenchymal cells and progenitors accessing the site<sup>(3–5)</sup>. Although progenitor cells' presence improves filling defects, studies have shown the quality of newly formed cartilaginous tissue is often fibrous over hyaline<sup>(3, 6, 7)</sup>. Accordingly, various growth factors (e.g., BMP7, BMP2, TGF $\beta$  and PRP) are applied in combination(s) with microfracture treatment to support the formation of hyaline cartilage regeneration<sup>(8–11)</sup>. Despite surgical technical advancements, improving the microfracture treatment's long-term outcome remains a challenge<sup>(4)</sup>. It's reported poor outcomes in 46% of patients 10–14 years post-surgery, with 39% of cohorts required additional surgical procedures following the original microfracture surgery<sup>(12)</sup>.

One of the growth factors, well-known anabolic effect on cartilage is fibroblast growth factor-18 (FGF18)<sup>(13–17)</sup>. FGF18 is a member of the fibroblast growth factor family playing a central role in skeletal growth and development<sup>(18–21)</sup>. Previous studies supported a role for FGF18 in chondrocyte proliferation, differentiation and cartilage matrix hemostasis. These studies demonstrated FGF18 increases collagen type II, glycosaminoglycan, and chondroitin sulfate expression and reduces collagen type II breakdown following cartilage injury<sup>(22, 14, 18, 15)</sup>.

Additionally, intra-articular injection of FGF18 in a rat osteoarthritis model reduced cartilage degeneration, induced new cartilage formation, and indicated a potent *in vivo* anabolic effect for FGF18<sup>(23)</sup>. This potential capability of FGF18 and the necessity for new and effective Disease-Modifying Osteoarthritis Drugs (DMOADs) inspired the development of sprifermin, a truncated recombinant human FGF18 (Merck KGaA, Darmstadt, Germany). *In vitro* experiments utilizing sprifermin have demonstrated an improvement in collagen type II:I ratio and hyaline cartilage matrix formation and revealed a “hit and run” mode of action for sprifermin<sup>(24)</sup>. In an *ex vivo* study, Sennet and colleagues showed sprifermin could increase collagen content and adhesive strength leading to better cartilage-cartilage integration and superior repair of a defect<sup>(25)</sup>. Sprifermin is currently in phase two of clinical trials for the treatment of knee osteoarthritis. A 12-months clinical study on 168 patients showed that sprifermin treatment was associated with statistically significant, dose-dependent improvement of lateral femorotibial cartilage thickness. This study also demonstrated a significant decrease in pain scores in patients who received sprifermin<sup>(26)</sup>. In the report of a recent 2-years clinical study, MRI results showed significant dose-

dependent modification of cartilage thickness in the total femorotibial joint, medial and lateral femorotibial compartments, and central medial and central lateral sub-regions<sup>(27)</sup>. Dahlberg *et al.* study on 55 patients scheduled for total knee replacement detected no systemic effect, acute inflammation, or safety concerns following intra-articular sprifermin injections<sup>(28)</sup>. Two animal studies on an ovine model supported the beneficial effect of intra-articular sprifermin treatment on cartilage repair following microfracture surgery, one showing an improvement in cartilage defect fill, and collagen type II expression in sprifermin treated ovine joints<sup>(29)</sup> and another showing enhancement in weight-bearing, histology scores and collagen type II expression following sprifermin treatment<sup>(30)</sup>.

The results of pre-clinical animal studies can best be extrapolated to a human condition in an appropriate animal models that more closely represents the human condition. Horses are considered as an excellent animal model for pre-clinical evaluation of new cartilage repair techniques and technologies<sup>(31, 32)</sup>.

In the present study, an equine animal model was used to investigate the effect of a three-dose intra-articular injection treatment regimen of sprifermin on the outcome of microfracture in a cartilage defect model (Fig. 1). Treatment with sprifermin was well-tolerated and safe, and by performing antemortem and postmortem evaluations, we detected a significant improvement in functional and structural aspects of the cartilage repair tissue as a result of sprifermin treatment.

## Methods

### Animals

Eighteen mixed gender healthy horses (age range 2–7 years) were enrolled in the study approved by the University of Pennsylvania Animal Care and Use Committee. All horses underwent physical and lameness examinations, including radiographic evaluation of all four fetlocks (metacarpophalangeal and metatarsophalangeal), joints prior to study inclusion.

### Surgical Technique

On day 0, each horse was placed under general anesthesia in right lateral recumbency for arthroscopy of all four fetlock joints. Arthroscopic portals were created in the palmar aspect of either the right or left metacarpophalangeal joint. A 15 mm circumferential full-thickness articular cartilage defect was created using a combination of an arthroscopic burr and curettes on the central dorsal aspect of the lateral proximal sesamoid bone. The defect extended approximately 2 mm from the most distal aspect of the bone to approximately 2 mm from the bone's abaxial border to the size of 15 mm. Discs made of the radiographic film were used as templates to ensure uniform size defects (Fig. 1A). A 45 or a 90-degree calibrated awl was used to micropick 25–30 locations within the defect. Arthroscopy portals were made as previously described in the contralateral metacarpophalangeal joint and the left plantar medial and right plantar lateral metatarsophalangeal joints. A cartilage defect was created in the lateral proximal sesamoid bones and micropicked as previously described in 3 out of four fetlock joints. One fetlock joint had a sham procedure where no defect was created and served as the control limb.

Animals were placed in their assigned stall (3.65 x 3.65 M) for the two initial weeks postoperatively and transitioned to free paddock turnout from weeks 3–12 postoperatively. A second look arthroscopy was performed on week 12. All animals were humanely euthanized at 24 weeks with an overdose of sodium pentobarbital. All four limbs were harvested for postmortem analysis.

### Treatment Groups

The weekly consecutive intra-articular medication of the testing article was performed from weeks 3–5. One joint each was medicated with 20 mg hyaluronan (Hylartin V®, Pfizer, New York, NY), 2 ml of 0.9% sterile sodium chloride (placebo), or one of three doses of sprifermin (10 µg, 30 µg and 100 µg). Six horses were randomly assigned to each dose-treatment group for a total of 18 horses (Fig. 1B). The treatment regime was based on the intended route of administration of the potential therapeutic in humans <sup>(26)</sup>.

### Methods: Primary Endpoints

**Histology**—Cartilage samples were harvested from the control, lesion, and kissing region of fetlocks. Samples decalcified, dehydrated, and paraffin-embedded before being cut into 7 mm sections and stained using Safranin O/Fast green. The slides were scanned on the Aperio ImageScope (Leica, Wetzlar, Germany) at 20 x, and 5 mm wide regions of interest were cropped and modified ICRSII scoring <sup>(33)</sup> was conducted by six independent observers blinded to treatment protocol using ten different metrics: (1) matrix staining, (2) cellularity, (3) superficial zone clustering, (4) middle-deep zone clustering, (5) surface architecture, (6) subchondral bone involvement, (7) lesion intensity, (8) superficial zone assessment, (9) middle-deep zone assessment, and (10) overall assessment. To evaluate cell proliferation, the number of chondrocytes were counted in each area using three regions of interest and manual counting.

**RNA Isolation and Real-Time PCR**—Cartilage samples were harvested from the lesion, peri-lesion, kissing region, and control. For RNA isolation, we used a Trizol based Qiagen miRNeasy micro kit. Two hundred µg of each RNA was used to synthesize cDNA using iScript™ (Bio-Rad, Hercules, CA). Real-time PCR was performed using a Fluidigm Biomark™ HD platform (Fluidigm, San Francisco, CA) and equine specific TaqMan® assays (Applied Biosystems, Thermo Fisher Scientific) probes. Before the Biomark™ assay, cDNA samples were pre-amplified for 12 cycles using a mix of Fluidigm PreAmp master-mix and pool of TaqMan® assays. The geometric mean of CT values from five different house-keeping genes (GAPDH, GUSB, ACTB, B2M, and SDHA) was used to measure the relative expression of genes of interest.

### Methods: Secondary Endpoints

**Clinical Assessment**—The lameness examinations performed at weeks 0, 3, 4, 5, 10, 12, 14, 18, 22, and 24 by a single-blinded observer board certified in large animal surgery. Lameness was graded on a standardized scale of 0–5, according to the American Association of Equine Practitioners guideline on a straight line and a circle. Fetlock flexion tests, as a subjective measure of pain and inflammation, were graded separately on a scale of 0–3 <sup>(34)</sup>.

**Synovial Fluid Analysis**—Synovial fluid was obtained from all four fetlock joints at weeks 0, 3, 4, 5, 10, 12, 14, 18, 22, and 24. Color, clarity, total protein (TP) concentration, and white blood cell (WBC) count were determined via routine methods.

**Second Look Arthroscopy**—Arthroscopic evaluation of the cartilage defect was performed at 12 weeks and videos reviewed by two blinded observers who scored the cartilage for: the tissue color, the surface integrity, and the degree of coverage; all on a scale of 1–5 (1 represented severe change and 5 was normal; Table S1) adopted from established scoring methods<sup>(35, 36)</sup>.

**Gross Joint Evaluation**—The fetlocks were disarticulated and digital photographs were obtained. The synovial membrane, joint capsule, and all articulating surfaces within the operated joints were examined and macroscopically evaluated and scored (Table S2) by two blinded observers using a previously established scoring system<sup>(35, 37, 36)</sup>.

**Radiographs**—Survey radiographs (Lateral-medial, dorsolateral/palmaromedial oblique, dorsomedial/palmarolateral oblique, and Dorsopalmar/plantar) of all joints were obtained following enrollment in the study, at 12 weeks postoperatively and termination (week 24). Two blinded observers evaluated and scored the radiographs for: peri-articular soft tissue swelling, soft tissue mineralization, and development of enthesophytes and osteophytes on a scale of 1–5 (1 represented severe change and 5 was normal; Table S3). The scoring system was adapted from Boyce *et al.*, 2013<sup>(38)</sup>.

**Computed Tomography**—Computed tomographic (CT) evaluation was performed with a portable 8-slice CT scanner (CereTom™ OTOScan, NeuroLogica, Danvers, MA) on all four fetlocks of all horses. Initial images were obtained at 2.5 mm slice thickness and reconstructed to 1.25 mm. Images were viewed on Osirix imaging software and graded by two blinded observers on a scale of 1–5, with a score of 1 being most severe (Table S4)<sup>(39)</sup>.

## Statistical Analysis

For gene expression and histology data, a non-parametric Mann-Whitney test was applied to determine the statistically significant gene expression differences between groups. The study is not powered for statistical analysis of the secondary endpoints. Therefore, the sprifermin groups were combined to assess a putative overall effect. In the case of data from second-look arthroscopy, radiography, CT, and gross evaluation, a non-parametric Kruskal-Wallis with Dunn's multiple comparison test is used to determine statistical significance within and between groups. For percentage benefits, scores from placebo, HA, and sprifermin treatment groups were compared to those from sham (100% benefit), and no statistical analysis was performed for these under-power measures.  $P < 0.05$  was accepted as significant in all analyses. No data imputation or baseline adjustments were implemented. Normality of data was evaluated by D'Agostino and Pearson test, Shapiro-Wilks test and QQ plots. GraphPad Prism 8 statistical software (GraphPad Software, Inc, La Jolla, CA) was used for data analysis.

## Results

### Results: Primary Endpoints

As primary endpoints, we choose the structural elements of histology and gene expression of the constitutive cartilage extracellular matrix and those related to the catabolic activity.

### Histological Evaluation

Histological evaluation of samples from three regions of interest (lesion, kissing region, opposite facing cartilage to the lesion, and control; Fig. 2A) showed significant improvement in several metrics resulting from sprifermin treatment.

In lesion, all placebo, HA, and sprifermin treated groups showed a fibrotic non-cartilaginous repair tissue, and their overall assessment was significantly deteriorated (Fig. 2D). We detected the most marked changes in the kissing region, where both 10 µg and 100 µg sprifermin groups showed an improvement in repair tissue (Fig. S1).

In the kissing region, 100 µg sprifermin caused significant improvement in surface architecture ( $93 \pm 4.33$  versus  $71.34 \pm 26.63$ ,  $p = 0.021$ ; Fig. S1E), decrease in the lesion intensity ( $91.94 \pm 11.71$  versus  $73.48 \pm 25.94$ ,  $p = 0.015$ ; Fig. S1G (scores and the lesion intensity are inversely related), and a nearly to significant improvement in the overall assessment ( $p = 0.057$ ; Fig. 2E) compared to the placebo. In the same region, 10 µg sprifermin significantly associated with improved surface architecture (sprifermin  $93.98 \pm 4.11$  versus placebo  $71.34 \pm 26.63$ ,  $p = 0.009$ ; Fig S 1E) and five out of six animals showed improvement in overall assessment when compared to placebo (Fig 2E). For the kissing region in the 30 µg sprifermin group, there was an opposite trend detected ( $p < 0.05$ ) with reduced cellularity, increased clustering and disrupted surface architecture when compared to sham joints (Fig. S1).

In control regions, except for a significant decrease in the overall assessment (Fig. 2C) and cellularity scores following treatment with 10 µg sprifermin, and a decrease in surface architecture score in 30 µg group, other metrics for 10 µg and 30 µg groups and all metrics for 100 µg group was comparable with sham. In addition, in lesion, kissing regions, and control groups, sprifermin treatment increased the average cell number. This increase was significant in the lesion of the 10 µg group; Fig. S1, K to M).

### Gene Expression

We evaluated gene expression in three regions: lesion, peri-lesion, and kissing region (Fig. 2A). In the peri-lesion of the 100 µg sprifermin group, there was a significant increase in aggrecan ( $p < 0.05$ ) and COMP ( $p < 0.01$ ) expression compared to HA and placebo groups (Fig. 3A and C). In the same treatment group, the average expression of collagen type II increased (100 µg sprifermin  $4885 \pm 3053$  versus placebo  $3031 \pm 2672$ ) and 5 out of 6 animals showed an improvement in collagen type II expression when compared to the average gene expression in placebo and HA groups (Fig. 3B). In the case of collagen type I expression, we detected a significant decrease compared to HA and placebo treatment groups (Collagen

type I  $1.068 \pm 0.57$  versus HA  $11.78 \pm 8.29$  and placebo  $20.64 \pm 27.63$ ,  $p = 0.0058$  and  $p = 0.018$  respectively; Fig. 3D).

In kissing regions, we detected a dose-dependent increase in average aggrecan, collagen type II, and COMP expression with the highest expression in 100  $\mu\text{g}$  group (Fig. 3E to G). In 100  $\mu\text{g}$  group, COMP expression showed a near to significant ( $p = 0.055$ ) and significant ( $p = 0.018$ ) increase compared to placebo and HA treated joints. Although we did not detect any significant changes in collagen type I expression, all animals except one showed a decrease in gene expression compared to the average of the gene expression in placebo and HA groups (0.0578 and 1.001 respectively; Fig. 3H).

In 100  $\mu\text{g}$  sprifermin treated lesions, when compared to placebo, there was an increase in the level of aggrecan, collagen type II, and COMP expression and a decrease in the level of collagen type I expression; however, these changes were not significant ( $p = 0.453$ ,  $0.922$ ,  $0.103$ , and  $0.136$  respectively; Fig. 3I to L). Five out of six animals treated with 100  $\mu\text{g}$  sprifermin showed an improvement (reduction) in collagen type I expression compared to the average gene expression in placebo and HA groups (average gene expression 38.9 and 31.32 respectively; Fig. 3L). Regarding the control cartilage samples, there were no relative changes in gene expression compared to the sham, except for an increase in collagen type II expression in 30  $\mu\text{g}$  and 100  $\mu\text{g}$  sprifermin ( $p = 0.001$  and  $p = 0.055$  respectively; data not shown).

## Results: Secondary Endpoints

In order to assess relevant clinical measurements and more functional outcomes, we performed following endpoint measurements.

### Clinical Assessments

Recovery from general anesthesia was without incident. For lameness and flexion assessment, looking at week by week results and combining scores from all sprifermin treated animals, scores peaked in the early postoperative phase and again after the second look arthroscopy at week twelve. This secondary peak was more prominent in the placebo-treated group (Fig. S2A and B). In addition, comparing sprifermin to HA treatment, scores from sprifermin treated joints were closer to sham values (Fig. S2A and B). We observed a gradual improvement in lameness and flexion test scores, and at time points after week 14, improvement in scores reached statistical significance ( $p < 0.05$ ; Fig. S2C and D). When the lameness sum scores for the whole duration of this study, it was seen that no single dose of sprifermin was superior to placebo treatment (Fig. 4A), but the combined results of three doses of sprifermin showed a significant improvement in lameness scores ( $2.5 \pm 3.777$  and  $6.30 \pm 5.51$ ,  $p = 0.046$ ; Fig. 4B). In the matter of flexion test, we observed a near to significant improvement when we combined results from various sprifermin dose treatment groups (sprifermin  $3.389 \pm 6.48$ , placebo  $7.667 \pm 6.851$ ,  $p = 0.053$ ; Fig. 4D).

### Synovial Fluid Analysis

There was no effect of treatment with sprifermin, HA, or placebo on total synovial fluid white cell counts or total protein (Fig. S2E and F).

## Second Look Arthroscopy and Gross Evaluation

Twelve weeks post-surgery, arthroscopic evaluation demonstrated a significant improvement in cartilage defect healing in joints treated with sprifermin compared to joints treated with HA or placebo (sprifermin  $10.19 \pm 2.71$  versus placebo  $9.16 \pm 2.93$ ,  $p=0.02$ , Fig. 5B). There was no significant difference between groups when looking at individual doses of sprifermin or between HA and placebo-treated groups (Fig. 5A). Evaluation of sub-scores showed significantly superior surface texture ( $p=0.05$ ) of sprifermin treated joints (Fig. 5C and S3F). Besides, treatment with 10  $\mu\text{g}$ , 30  $\mu\text{g}$  or 100  $\mu\text{g}$  sprifermin demonstrated a higher benefit when compared to HA treatment (37.6%, 24.7%, and 34.1% respectively versus 17.6%).

Postmortem evaluation revealed that treatment with no single dose of sprifermin resulted in a significant improvement in overall gross morphology (Fig. 5D). When we combined results from various sprifermin treatment groups, a near significant improvement was detected ( $22.42 \pm 3.40$  versus  $20.03 \pm 3.09$ ,  $p=0.060$ ; Fig. 5E). In an analysis of multiple sub-scores, we detected a significant ( $p=0.039$ ) and a near to significant ( $p=0.058$ ) improvement in cartilage surface and defect fill, respectively (Fig. 5F, S 4I and K).

We detected no significant difference between HA and placebo-treated limbs. The percentage benefit evaluation showed a more considerable and inversely dose-related benefit in sprifermin treatment than HA (ranged from 37.4% to 21.4% versus 0.53%).

## Radiographic and Computed Tomography Scores

Radiographs and CT examination showed decreased osteoarthritic changes in sprifermin treated joints compared to placebo and HA (Fig. 6).

At week 12, radiography scores were significantly improved in high dose (100  $\mu\text{g}$ ) sprifermin ( $p<0.05$ ) or when we combined the scores from three sprifermin dose-treatment groups ( $p<0.01$ ; Fig. 6B and C). The same significant improvement in radiographic scores of the 100  $\mu\text{g}$  group was detected at week 24 post-surgery ( $p=0.016$ ; Fig. 6D), and combined sprifermin scores were also significantly improved ( $8.31 \pm 0.941$  versus  $17.39 \pm 0.883$ ,  $p=0.011$ ; Fig. 6E). Peri-articular soft tissue swelling and soft tissue mineralization were the main radiographic features improved due to sprifermin treatment ( $p=0.024$  and  $0.064$ , respectively (Fig. S5E, and F). There was an increased benefit in low dose (10  $\mu\text{g}$ ) and high dose (100  $\mu\text{g}$ ) sprifermin compared to HA (48.6% and 70% respectively versus 25.7%).

At week 24, CT scores of combined sprifermin showed significantly less osteoarthritic change than placebo ( $20.39 \pm 2.38$  versus  $18.53 \pm 2.09$ ,  $p=0.043$ ; Fig. 6H). Evaluation of sub-scores showed reduced osteophyte development in sprifermin treated limbs at 24 weeks ( $p<0.01$ ) compared to HA and placebo-treated joints (Fig. S 6G). Additionally, treatment with any of three doses of sprifermin had a more notable benefit when compared to HA (ranged from 26.3% to 36.4% versus 3.3%).

## Discussion

Development of DMOADs continues to be a challenge in orthopedics; many agents have failed in clinical trials, and diseases such as osteoarthritis that often result from earlier joint



injuries remains a profound clinical problem. A common approach to many cartilage injuries is the use of microfracture and in this study we explored the combination of microfracture and the modified FGF-18, sprifermin in an equine model of cartilage injury. In many *in vitro* studies sprifermin has been shown to have beneficial effects on cartilage biosynthesis, integration and supporting mechanical properties<sup>(24, 40–42, 25)</sup>. In human clinical studies, sprifermin has been shown to be safe and effective at some aspects of osteoarthritis<sup>(28, 27, 26)</sup>. Further investigation in a large animal model is critical in evaluating sprifermin as a potential DMOAD since more controlled and early disease can be evaluated. In the present study, using an equine animal model, we demonstrated that applying sprifermin in conjunction with microfracture treatment can improve the outcome. This result is consistent with *in vivo* findings in other animal models and *in vitro* and *ex vivo* studies that suggest an anabolic role for sprifermin in cartilage healing and hemostasis<sup>(15, 24, 30, 29, 25)</sup>.

Comparing various animal models, horses are considered excellent models for human mimicry in regard to cartilage studies<sup>(31, 32)</sup>. Poor intrinsic regenerative capacity, large easily sampled joints, and thick articular cartilage in horses make their articular cartilage defects comparable to the same lesions in humans and allow comprehensive cartilage studies to test efficacy and safety of new cartilage treatments. In addition, horses, like humans, suffer from sports injuries, and as a result, articular cartilage injury treatments and surgeries are better understood in horses than other animal models<sup>(43)</sup>.

In this study, we examined the impact of sprifermin in both functional and structural aspects of cartilage healing. In sprifermin treated joints, we detected a significant improvement in lameness; arthroscopic evaluation showed superior quality and quantity of the repair tissue, and both radiographic and CT scan imaging showed mitigated pathology. In postmortem evaluation of the repair tissue, we detected an improvement in the defect site's gross morphology, the overall histological assessment of the kissing region, and the expression of the constitutive genes. For the most part, no single dose of sprifermin showed a statistically significant advantage over placebo or HA. However, when we combined scores from three dose-treatment groups, changes were significant. In addition, looking closely at our non-significant changes in sprifermin scores, we observed that in most cases, at least 50–60% of subjects showed an improvement compared to the average placebo scores. This lack of significance can be due to the small per group sample size (n=6) that is a known limitation when using an equine model<sup>(31)</sup>. We compared the outcome of the sprifermin treatment to HA treatment, as a common osteoarthritis intraarticular therapeutics, and the majority of tests detected higher benefit associated with sprifermin.

Through our antemortem and postmortem tests, we observed a concentration-dependent benefit in sprifermin treatment with the highest benefit in 100 µg injections except for lameness and flexion test scores. Increased lameness in high dose sprifermin group may be a consequence of an acute and transient inflammatory reaction (joint stiffness and arthralgia) that was previously observed in human clinical trials with the administration of high dose sprifermin (100 or 300 µg)<sup>(28, 26)</sup>. Another limitation was observed in our early clinical assessment. For this study, horses were not randomized based on surgical status. As a result, the placebo cohort had a slightly higher lameness (not statistically significant) immediately post-surgery that was revealed to us at the end of the study after unblinding. Lameness and

flexion test scores were not adjusted to the baseline. At later time points, the slight initial dissimilarity expanded and we detected a significant improvement in sprifermin treated joints.

In addition to the efficiency of sprifermin on the improvement of cartilage healing, this study, notably, detected no adverse effects following sprifermin treatment. This finding is also consistent with the approved safety of sprifermin during human clinical trials<sup>(28, 26)</sup>. We also detected that the unique three intermittent intraarticular sprifermin injections alter gene expression in chondrocytes (e.g., increase in type II collagen and aggrecan expression and decrease in collagen type I expression) at the repair site and areas in direct contact with it. We assume that such a response is mediated through sprifermin binding to its functional receptor, FGFR3, and activation of ERK1/2 signaling pathways. It has been shown that this pathway's blockade can inhibit the sprifermin impact<sup>(14, 24)</sup>. Previous studies have suggested the potential benefit of FGF18-FGFR3 binding and an increase in FGFR3 expression for the improvement of articular cartilage integrity<sup>(44, 45)</sup>. Notably, we detected an increase in average FGFR3 gene expression in all three regions of interest following 100 µg sprifermin treatment. Although an increase in gene expression was not statistically significant, five animals out of six showed improvement in FGFR3 expression in the peri-lesion and kissing region compared to the placebo group's average gene expression (Fig S6, I and J).

Although for an equine study, this study was conducted with a large number of subjects, it still was likely underpowered. While this was a considerably protracted evaluation timeframe, more extensive studies with a higher number of subjects and even longer durations will be critical to investigate sprifermin's long term effect on cartilage healing and functional restoration. Wilke *et al.* recommend at least eight months to assess a treatment outcome in an equine cartilage defect model<sup>(46)</sup>.

Despite such limitations, this study clearly shows how large animal studies can be additive to the body knowledge obtained from human clinical trials. In general large animals can be experimentally modified and earlier pathology and disease manifestations can be explored that are impossible in human studies. Large animal studies provide parallels to human studies by allowing better control over the injury and early interventions, and we can conduct postmortem evaluations. Future *in vivo* studies will be needed to understand the biomechanical benefits of sprifermin treatment and investigate the underlying mechanism of sprifermin effect on cartilage healing and clinically relevant function on a long term basis.

This study shows for the first time that intra-articular sprifermin enhances the effects of microfracture surgery in an equine model and identifies potential benefits from sprifermin treatment in early cartilage injuries in both veterinary and human medicine. Showing both functional and structural effects of sprifermin, this study represents a therapeutic advancement in treatments of cartilage injury and ultimately offsetting or treating osteoarthritis.

## Supplementary Material

Refer to Web version on PubMed Central for supplementary material.

## Acknowledgments

The authors gratefully acknowledge the advice and technical assistance of Ryan Smalley, Patrick Diviney, Dr. Bhavana Monhanraj, Hans Guehring, one of the authors, is a paid employee of Merck KGaA. This work was supported by a grant from Merck KGaA. Additional support was provided by the Department of Veteran's Affairs (I01 RX001213 and VA RR&D I01 RX001321) and the NIH-NIAMS via R01 AR071340 (GRD), and the Penn Center for Musculoskeletal Diseases Biomechanics and Histology Core (NIH NIAMS P30-AR069619).

## Abbreviations

<b>ACTB</b>	actin beta
<b>B2M</b>	beta-2 microglobulin
<b>BMP</b>	Bone morphogenic protein
<b>cDNA</b>	complementary deoxyribonucleic acid
<b>COMP</b>	cartilage oligomeric matrix protein
<b>CT scan</b>	Computed Tomography scan
<b>CT</b>	cycle threshold
<b>DLPMO</b>	dorsolateral/palmaromedial oblique
<b>DMOADs</b>	Disease Modifying Osteoarthritis Drugs
<b>DMPLO</b>	dorsomedial/palmarolateral oblique
<b>ERK</b>	extracellular receptor kinase
<b>FGF18</b>	fibroblast growth factor-18
<b>FGFR3</b>	fibroblast growth factor receptor 3
<b>GAPDH</b>	glyceraldehyde 3-phosphate dehydrogenase
<b>GUSB</b>	glucuronidase beta
<b>HA</b>	Hyaluronan
<b>LFTC</b>	lateral femorotibial compartment
<b>MFTC</b>	medial femorotibial compartments
<b>MFX</b>	microfracture
<b>MRI</b>	magnetic resonance imaging
<b>PCR</b>	polymerase chain reaction
<b>PRP</b>	Platelet-rich plasma

<b>PTOA</b>	post-traumatic osteoarthritis
<b>RNA</b>	ribonucleic acid
<b>SDHA</b>	succinate dehydrogenase complex flavoprotein subunit A
<b>TFTJ</b>	total femorotibial joint
<b>TGFβ</b>	transforming growth factor beta
<b>TP</b>	total protein
<b>WBC</b>	white blood cell

## References

1. Steadman JR, Briggs KK, Rodrigo JJ, et al. 2003. Outcomes of microfracture for traumatic chondral defects of the knee: average 11-year follow-up. *Arthroscopy* 19(5):477–484. [PubMed: 12724676]
2. Steadman JR, Rodkey WG, Briggs KK. 2010. Microfracture: Its History and Experience of the Developing Surgeon. *Cartilage* 1(2):78–86. [PubMed: 26069538]
3. Breinan HA, Martin SD, Hsu HP, Spector M. 2000. Healing of canine articular cartilage defects treated with microfracture, a type-II collagen matrix, or cultured autologous chondrocytes. *J Orthop Res* 18(5):781–789. [PubMed: 11117301]
4. Mithoefer K, McAdams T, Williams RJ, et al. 2009. Clinical efficacy of the microfracture technique for articular cartilage repair in the knee: an evidence-based systematic analysis. *Am J Sports Med* 37(10):2053–2063. [PubMed: 19251676]
5. Oussedik S, Tsitskaris K, Parker D. 2015. Treatment of articular cartilage lesions of the knee by microfracture or autologous chondrocyte implantation: a systematic review. *Arthroscopy* 31(4):732–744. [PubMed: 25660008]
6. Furukawa T, Eyre DR, Koide S, Glimcher MJ. 1980. Biochemical studies on repair cartilage resurfacing experimental defects in the rabbit knee. *J Bone Joint Surg Am* 62(1):79–89. [PubMed: 7351420]
7. Knutsen G, Engebretsen L, Ludvigsen TC, et al. 2004. Autologous chondrocyte implantation compared with microfracture in the knee. A randomized trial. *J Bone Joint Surg Am* 86(3):455–464. [PubMed: 14996869]
8. Guney A, Akar M, Karaman I, et al. 2015. Clinical outcomes of platelet rich plasma (PRP) as an adjunct to microfracture surgery in osteochondral lesions of the talus. *Knee Surg Sports Traumatol Arthrosc* 23(8):2384–2389. [PubMed: 24292979]
9. Kang SW, Bada LP, Kang CS, et al. 2008. Articular cartilage regeneration with microfracture and hyaluronic acid. *Biotechnol Lett* 30(3):435–439. [PubMed: 17973085]
10. Kuo AC, Rodrigo JJ, Reddi AH, et al. 2006. Microfracture and bone morphogenetic protein 7 (BMP-7) synergistically stimulate articular cartilage repair. *Osteoarthritis Cartilage* 14(11):1126–1135. [PubMed: 16765606]
11. Yang HS, La WG, Bhang SH, et al. 2011. Hyaline cartilage regeneration by combined therapy of microfracture and long-term bone morphogenetic protein-2 delivery. *Tissue Eng Part A* 17(13–14):1809–1818. [PubMed: 21366427]
12. Solheim E, Hegna J, Inderhaug E, et al. 2016. Results at 10–14 years after microfracture treatment of articular cartilage defects in the knee. *Knee Surg Sports Traumatol Arthrosc* 24(5):1587–1593. [PubMed: 25416965]
13. Correa D, Somoza RA, Lin P, et al. 2015. Sequential exposure to fibroblast growth factors (FGF) 2, 9 and 18 enhances hMSC chondrogenic differentiation. *Osteoarthritis Cartilage* 23(3):443–453. [PubMed: 25464167]
14. Davidson D, Blanc A, Filion D, et al. 2005. Fibroblast growth factor (FGF) 18 signals through FGF receptor 3 to promote chondrogenesis. *J Biol Chem* 280(21):20509–20515. [PubMed: 15781473]

15. Ellsworth JL, Berry J, Bukowski T, et al. 2002. Fibroblast growth factor-18 is a trophic factor for mature chondrocytes and their progenitors. *Osteoarthritis Cartilage* 10(4):308–320. [PubMed: 11950254]
16. Liu Z, Lavine KJ, Hung IH, Ornitz DM. 2007. FGF18 is required for early chondrocyte proliferation, hypertrophy and vascular invasion of the growth plate. *Dev Biol* 302(1):80–91. [PubMed: 17014841]
17. Ohbayashi N, Shibayama M, Kurotaki Y, et al. 2002. FGF18 is required for normal cell proliferation and differentiation during osteogenesis and chondrogenesis. *Genes Dev* 16(7):870–879. [PubMed: 11937494]
18. Ellman MB, Yan D, Ahmadinia K, et al. 2013. Fibroblast growth factor control of cartilage homeostasis. *J Cell Biochem* 114(4):735–742. [PubMed: 23060229]
19. Krejci P, Krakow D, Mekikian PB, Wilcox WR. 2007. Fibroblast growth factors 1, 2, 17, and 19 are the predominant FGF ligands expressed in human fetal growth plate cartilage. *Pediatr Res* 61(3):267–272. [PubMed: 17314681]
20. Naski MC, Colvin JS, Coffin JD, Ornitz DM. 1998. Repression of hedgehog signaling and BMP4 expression in growth plate cartilage by fibroblast growth factor receptor 3. *Development* 125(24):4977–4988. [PubMed: 9811582]
21. Yang W, Cao Y, Zhang Z, et al. 2018. Targeted delivery of FGF2 to subchondral bone enhanced the repair of articular cartilage defect. *Acta Biomater* 69:170–182. [PubMed: 29408545]
22. Barr L, Getgood A, Guehring H, et al. 2014. The effect of recombinant human fibroblast growth factor-18 on articular cartilage following single impact load. *J Orthop Res* 32(7):923–927. [PubMed: 24719286]
23. Moore EE, Bendele AM, Thompson DL, et al. 2005. Fibroblast growth factor-18 stimulates chondrogenesis and cartilage repair in a rat model of injury-induced osteoarthritis. *Osteoarthritis Cartilage* 13(7):623–631. [PubMed: 15896984]
24. Gigout A, Guehring H, Froemel D, et al. 2017. Sprifermin (rhFGF18) enables proliferation of chondrocytes producing a hyaline cartilage matrix. *Osteoarthritis Cartilage* 25(11):1858–1867. [PubMed: 28823647]
25. Sennett ML, Meloni GR, Farran AJE, et al. 2018. Sprifermin treatment enhances cartilage integration in an in vitro repair model. *J Orthop Res* 36(10):2648–2656. [PubMed: 29761549]
26. Lohmander LS, Hellot S, Dreher D, et al. 2014. Intraarticular sprifermin (recombinant human fibroblast growth factor 18) in knee osteoarthritis: a randomized, double-blind, placebo-controlled trial. *Arthritis Rheumatol* 66(7):1820–1831. [PubMed: 24740822]
27. Hochberg MC, Guermazi A, Guehring H, et al. 2019. Effect of Intra-Articular Sprifermin vs Placebo on Femorotibial Joint Cartilage Thickness in Patients With Osteoarthritis: The FORWARD Randomized Clinical Trial. *JAMA* 322(14):1360–1370. [PubMed: 31593273]
28. Dahlberg LE, Aydemir A, Muurahainen N, et al. 2016. A first-in-human, double-blind, randomised, placebo-controlled, dose ascending study of intra-articular rhFGF18 (sprifermin) in patients with advanced knee osteoarthritis. *Clin Exp Rheumatol* 34(3):445–450. [PubMed: 27050139]
29. Power J, Hernandez P, Guehring H, et al. 2014. Intra-articular injection of rhFGF-18 improves the healing in microfracture treated chondral defects in an ovine model. *J Orthop Res* 32(5):669–676. [PubMed: 24436147]
30. Howard D, Wardale J, Guehring H, Henson F. 2015. Delivering rhFGF-18 via a bilayer collagen membrane to enhance microfracture treatment of chondral defects in a large animal model. *J Orthop Res* 33(8):1120–1127. [PubMed: 25721940]
31. Chu CR, Szczodry M, Bruno S. 2010. Animal models for cartilage regeneration and repair. *Tissue Eng Part B Rev* 16(1):105–115. [PubMed: 19831641]
32. McIlwraith CW, Fortier LA, Frisbie DD, Nixon AJ. 2011. Equine Models of Articular Cartilage Repair. *Cartilage* 2(4):317–326. [PubMed: 26069590]
33. Mainil-Varlet P, Van Damme B, Nestic D, et al. 2010. A new histology scoring system for the assessment of the quality of human cartilage repair: ICRS II. *Am J Sports Med* 38(5):880–890. [PubMed: 20203290]

34. American Association of Equine Practitioners (AAEP). Lameness Exams: Evaluating the Lame Horse
35. Goebel L, Orth P, Muller A, et al. 2012. Experimental scoring systems for macroscopic articular cartilage repair correlate with the MOCART score assessed by a high-field MRI at 9.4 T-- comparative evaluation of five macroscopic scoring systems in a large animal cartilage defect model. *Osteoarthritis Cartilage* 20(9):1046–1055. [PubMed: 22698442]
36. van den Borne MP, Raijmakers NJ, Vanlauwe J, et al. 2007. International Cartilage Repair Society (ICRS) and Oswestry macroscopic cartilage evaluation scores validated for use in Autologous Chondrocyte Implantation (ACI) and microfracture. *Osteoarthritis Cartilage* 15(12):1397–1402. [PubMed: 17604187]
37. Little CB, Smith MM, Cake MA, et al. 2010. The OARSI histopathology initiative - recommendations for histological assessments of osteoarthritis in sheep and goats. *Osteoarthritis Cartilage* 18 Suppl 3:S80–92. [PubMed: 20864026]
38. Boyce MK, Trumble TN, Carlson CS, et al. 2013. Non-terminal animal model of post-traumatic osteoarthritis induced by acute joint injury. *Osteoarthritis Cartilage* 21(5):746–755. [PubMed: 23467035]
39. Cohen MM, Vela ND, Levine JE, Barnoy EA. 2015. Validating a new computed tomography atlas for grading ankle osteoarthritis. *J Foot Ankle Surg* 54(2):207–213. [PubMed: 25135101]
40. Meloni GR, Farran A, Mohanraj B, et al. 2019. Recombinant human FGF18 preserves depth-dependent mechanical inhomogeneity in articular cartilage. *Eur Cell Mater* 38:23–34. [PubMed: 31393594]
41. Reker D, Kjelgaard-Petersen CF, Siebuhr AS, et al. 2017. Sprifermin (rhFGF18) modulates extracellular matrix turnover in cartilage explants ex vivo. *J Transl Med* 15(1):250. [PubMed: 29233174]
42. Reker D, Siebuhr AS, Thudium CS, et al. 2020. Sprifermin (rhFGF18) versus vehicle induces a biphasic process of extracellular matrix remodeling in human knee OA articular cartilage ex vivo. *Sci Rep* 10(1):6011. [PubMed: 32265494]
43. Frisbie DD, Cross MW, McIlwraith CW. 2006. A comparative study of articular cartilage thickness in the stifle of animal species used in human pre-clinical studies compared to articular cartilage thickness in the human knee. *Vet Comp Orthop Traumatol* 19(3):142–146. [PubMed: 16971996]
44. Tang J, Su N, Zhou S, et al. 2016. Fibroblast Growth Factor Receptor 3 Inhibits Osteoarthritis Progression in the Knee Joints of Adult Mice. *Arthritis Rheumatol* 68(10):2432–2443. [PubMed: 27159076]
45. Valverde-Franco G, Binette JS, Li W, et al. 2006. Defects in articular cartilage metabolism and early arthritis in fibroblast growth factor receptor 3 deficient mice. *Hum Mol Genet* 15(11):1783–1792. [PubMed: 16624844]
46. Wilke MM, Nydam DV, Nixon AJ. 2007. Enhanced early chondrogenesis in articular defects following arthroscopic mesenchymal stem cell implantation in an equine model. *J Orthop Res* 25(7):913–925. [PubMed: 17405160]

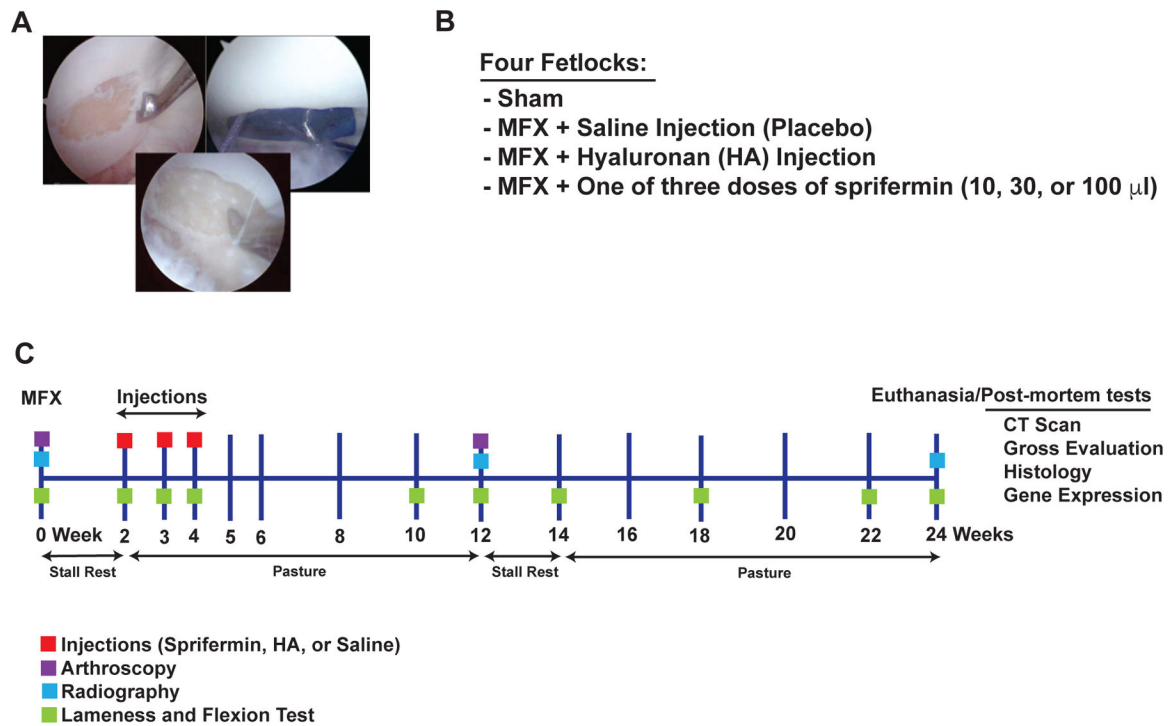


**Figure 1.**

Surgical technique, study design, and study time line

A 15 mm circumferential full thickness articular cartilage defect was created on the central dorsal aspect of the lateral proximal sesamoid bone (left). Radiographic film was used as a template to ensure the defects were of uniform size (right) and an awl was used to micropick 25–30 locations within the defect (bottom). **(B)** Four fetlocks of each animal were randomly assigned to one of the treatment groups. **(C)** Schematic overview of the study time line. MFX= microfracture treatment, HA= hyaluronan.

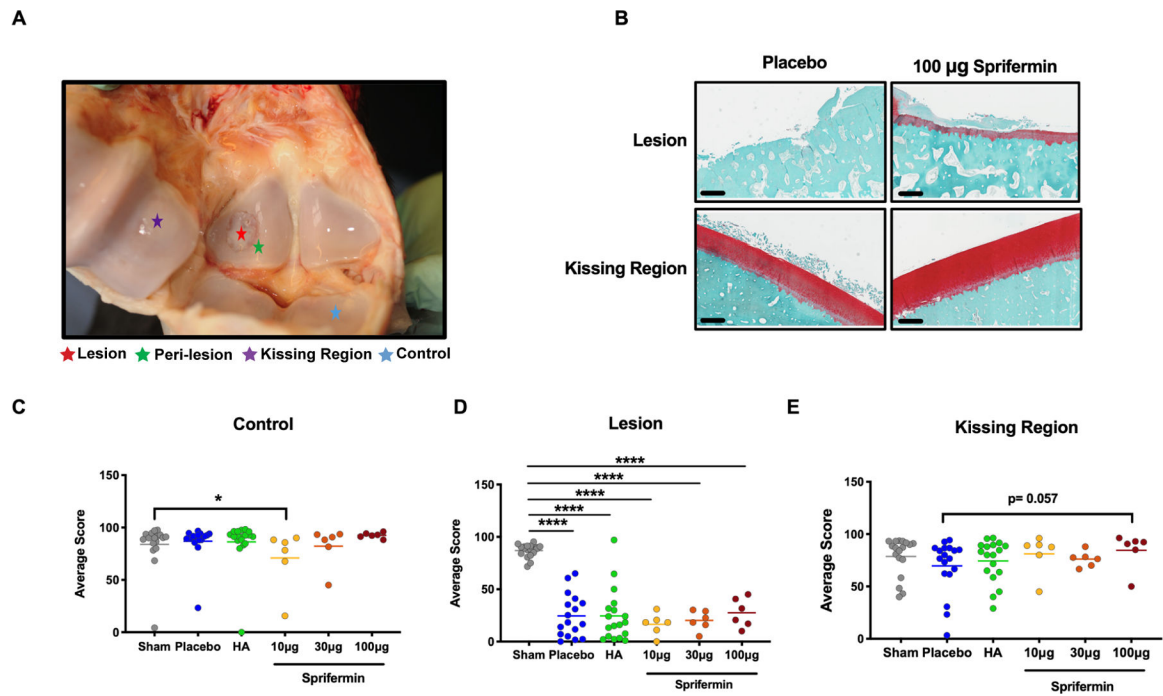


**Figure 2.** Histological Evaluation of fetlocks **(A)** Cartilage samples were harvested from four regions of interest inside fetlocks. **(B)** An example of the Safranin O/Fast Green staining in lesion and kissing region of placebo and 100 µg sprifermin treated fetlocks of an individual horse. 20x magnification images, scale bar = 500 µm. **(C)** Overall assessment of control, **(D)** Lesion, and **(E)** Kissing region compares scores in joints received HA or sprifermin treatment with sham and placebo treated joints. n= 6 or 18, \* $p < 0.05$  by un-paired Mann-Whitney test. In scatter plots, transvers lines represent median.



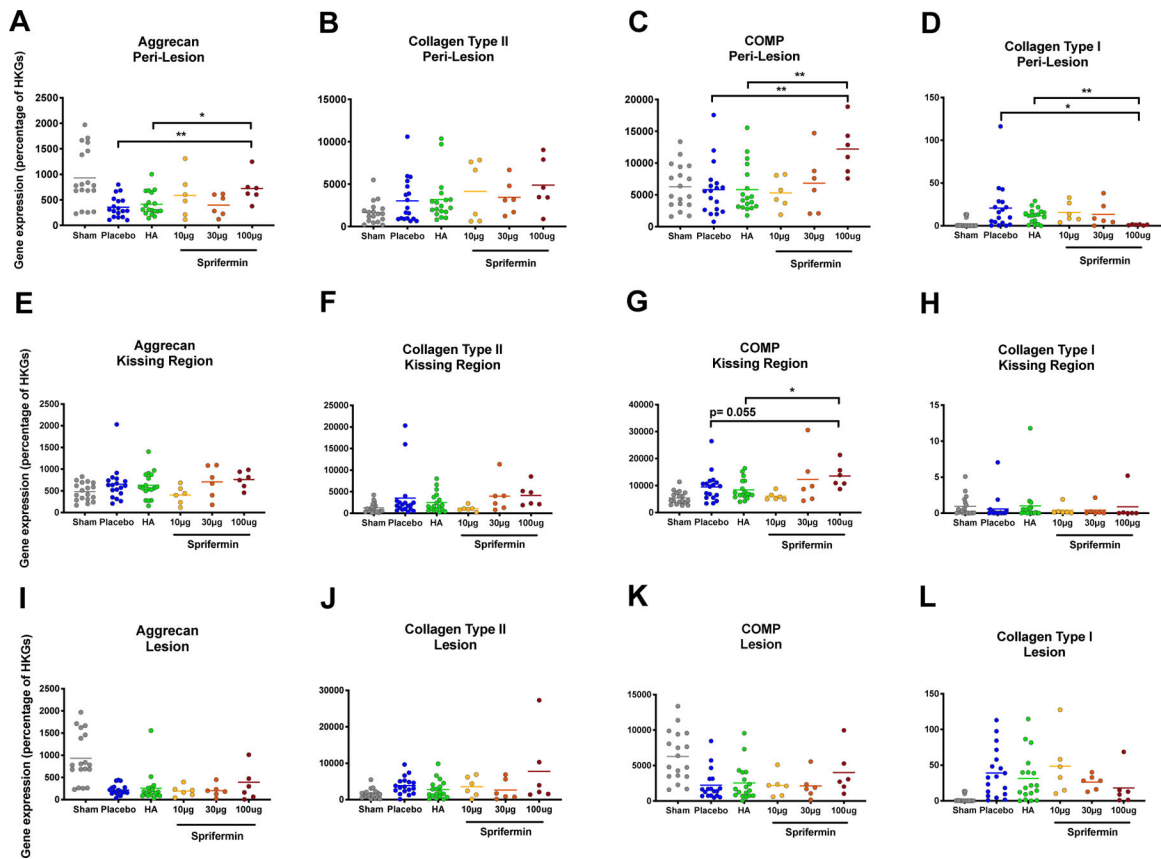


**Figure 3.**

Evaluation of gene expression in three regions of interest based on postmortem Real-Time PCR results (**A to D**) Aggrecan, Collagen type II, COMP, and Collagen type I expression in peri-lesion showed dose response changes in gene expression following sprifermin treatment. (**E to H**) Changes in gene expression in kissing region showed a significant and near to significant improvement in COMP expression. (**I to L**) Changes in gene expression in lesion showed a non-significant dose response to sprifermin treatment. Gene expression in sprifermin treated joints were compared to placebo or HA treatment groups using un-paired Mann-Whitney test.  $n=6$  or  $18$ ,  $*p<0.05$ ,  $**p<0.01$ . In scatter plots, transvers lines represent median.

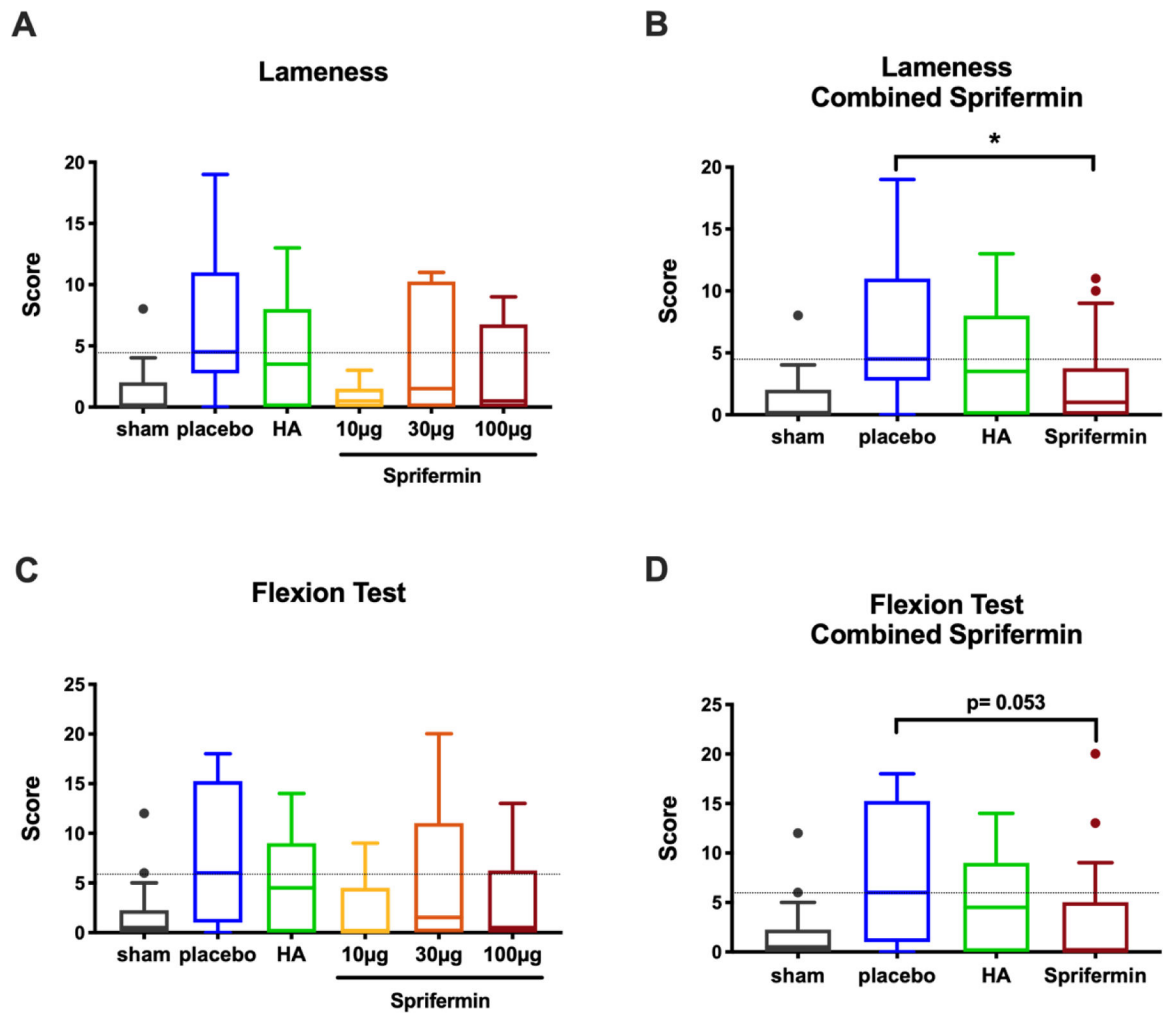


**Figure 4.** Clinical assessment via lameness and flexion tests. **(A)** An average of ten lameness scores for limbs treated with various doses of sprifermin, HA, or placebo. **(B)** Combined scores from three sprifermin dose-treatment groups showed a significant reduction in lameness when compared to the placebo. **(C)** An average of ten flexion test scores for limbs received various intraarticular treatments. **(D)** Combined scores from three dose-treatment groups showed near to significant reduction compared to the placebo. Dotted line indicates median of the placebo group.  $n=6$  or  $18$ ,  $*p<0.05$  by Kruskal-Wallis and Dunn's multiple comparison test. In boxed plots, transverse lines show median and error bars represent SEM.

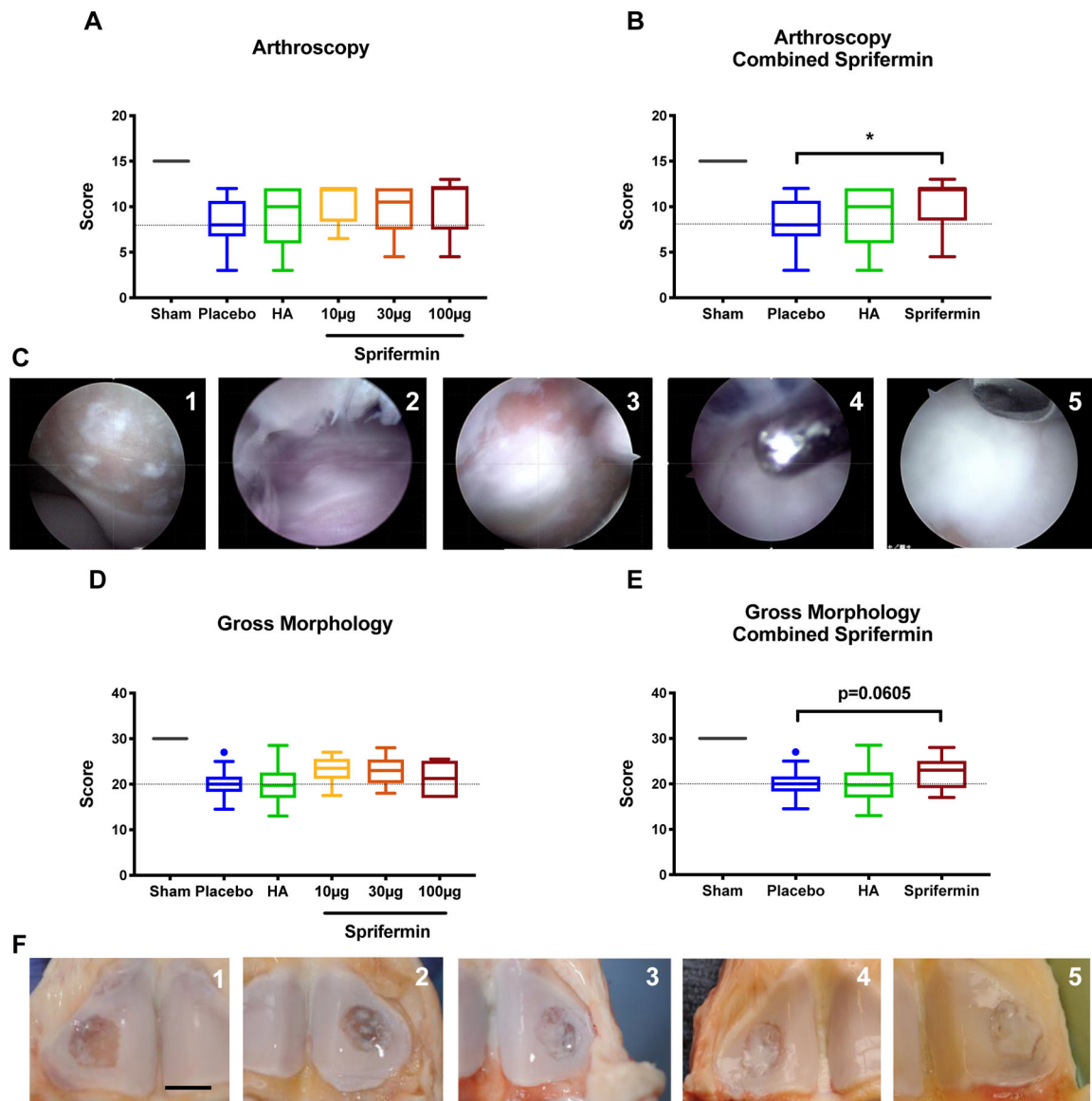


**Figure 5.**

Second look Arthroscopic evaluation of the defect site at 12 weeks post-surgery and postmortem gross evaluation (A) Sum-score of the three arthroscopic evaluation sub-scores showed no significant advantage in any single dose of sprifermin. (B) Arthroscopic evaluation sum-score of combined sprifermin groups was significantly higher than placebo. (C) Representative arthroscopic images for grade 1–5 of surface (D) Sum-scores of the six sub-scores showed no significant improvement in gross morphology following any of sprifermin doses. (E) Sum-scores showed a nearly significant improvement in gross morphology when scores from three sprifermin doses were combined. (F) Representative images for grade 1–5 of surface and defect fill, Scale bar=15mm. Dotted line indicates median of the placebo group. n= 6 or 18, \* $p < 0.05$  by Kruskal-Wallis and Dunn's multiple comparison test. In boxed plots, transverse lines show median and error bars represent SEM.

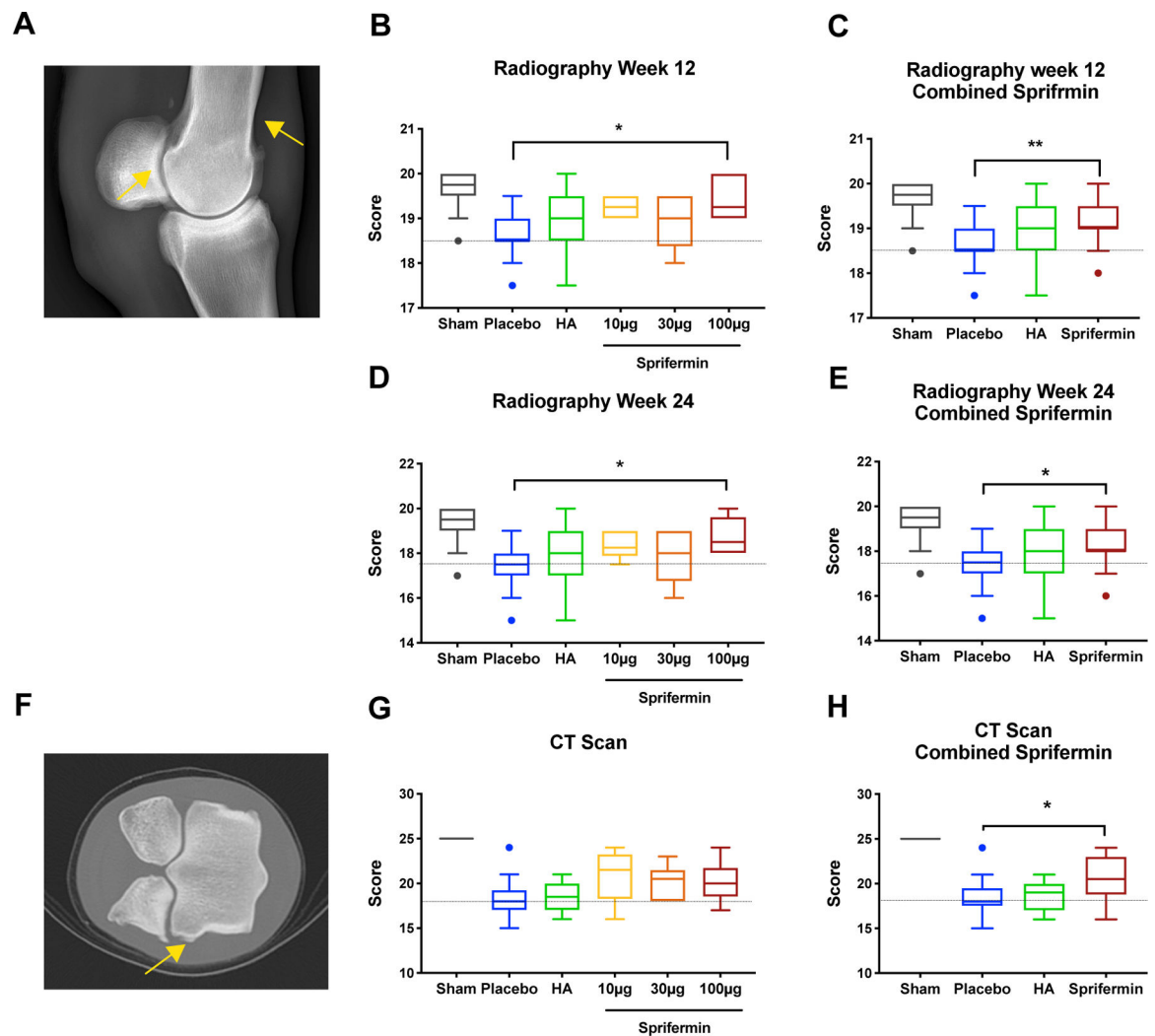


**Figure 6.** Radiographic and CT scan evaluation of fetlocks (A) Radiograph of a fetlock 24 weeks post-surgery showed formation of osteophytes (yellow arrows). (B) Evaluation of sum-scores of four radiography sub-scores showed a significant improvement in 100 µg sprifermin treatment group at 12 weeks post-surgery. (C) Combined scores from sprifermin treatment groups at 12 weeks post-surgery showed a significant improvement in radiographic scores. (D) Evaluation of sum-scores of four radiography sub-scores showed a significant improvement in 100 µg sprifermin treatment group 24 weeks post-surgery when compared to placebo. (E) Combined scores from sprifermin treatment groups at week 24 showed a significant improvement in radiographic scores. (F) CT-Scan image of a fetlock showed formation of osteophytes (yellow arrow). (G) Evaluation of sum-score of four CT scan sub-scores did not detect a significant improvement following treatment with any of three doses of sprifermin. (H) Sum-score of combined sprifermin groups showed a significant improvement compared to placebo. Dotted line indicates median of the placebo group. n=

6 or 18,  $*p < 0.05$  by Kruskal-Wallis and Dunn's multiple comparison test. In boxed plots, transverse lines show median and error bars represent SEM.

Author Manuscript

Author Manuscript

Author Manuscript

Author Manuscript